Supporting Information

Dual Aptamer Modified Dendrigraft Poly-L-lysines Nanoparticle for Overcoming Multi-drug Resistance through Mitochondrial Targeting

Huachao Chen [a,b,†], Jiangwei Tian [b,†], Danyang Liu [a], Weijiang He [a] and Zijian Guo [a,*]

Supplementary figures

1. **Figure S1.** Job plot for the determination of the the Dox/Duplex binding ratio.
2. **Figure S2.** Long-term-stability study of Dox/Mito-DGL in RPMI 1640 or DMEM with 10% FBS.
3. **Figure S3.** Confocal fluorescence imaging of HeLa cells incubated with 50 μg mL^{-1} Dox/Mito-DGL for 3 h and 6 h.
4. **Figure S4.** Colocalization images of Dox/Mito-DGL in PC3 cells.
5. **Figure S5.** Confocal fluorescence images of the intracellular release of Dox from Dox/Mito-DGL.
6. **Figure S6.** MTT assay of PC3 cells in the presence of different concentrations of Mito-DGL, Dox/Mito-cDGL, free Dox, and Dox/Mito-DGL.
7. **Figure S7.** MTT assay of MCF-7 cells in the presence of different concentrations of Mito-DGL, Dox/Mito-cDGL, free Dox, and Dox/Mito-DGL.
8. **Figure S8.** MTT assay of MCF-7/ADR cells in the presence of different concentrations of Mito-DGL, Dox/Mito-cDGL, free Dox, and Dox/Mito-DGL.
9. **Figure S9.** Confocal fluorescence images of apoptosis by the JC-1 assay in drug-sensitive HeLa and drug resistance HeLa/ADR cells.
10. **Figure S10.** MTT assay of HeLa/ADR cells in the presence of different concentrations of Mito-DGL, Dox/Mito-cDGL, free Dox, and Dox/Mito-DGL.

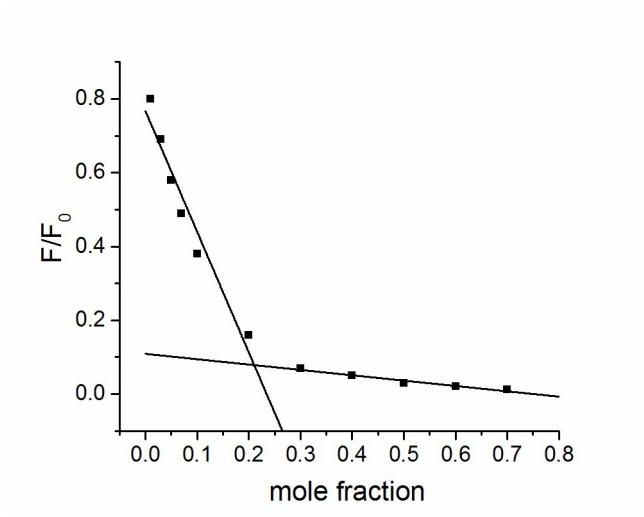

Figure S1. Job plot for the determination of the the Dox/Duplex binding ratio. The x-axis of the Job plot is the ratio of the concentration of Duplex to the total concentration of Duplex and Dox. The sum of [Duplex] and [Dox] was held constant at 5 μM. F_0 and F are the fluorescence intensities in the absence and presence of duplex, respectively.

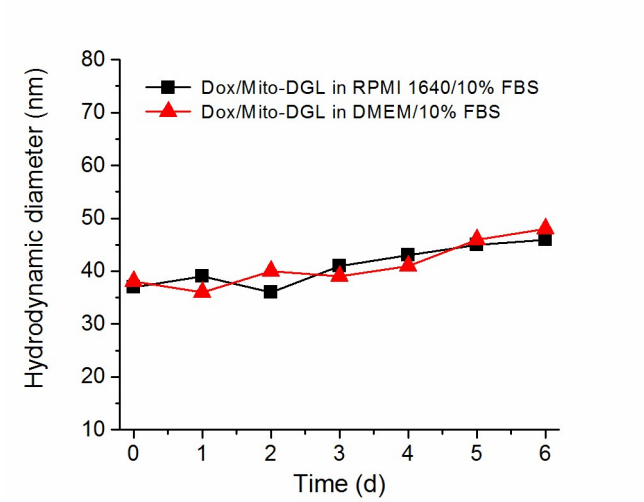

Figure S2. Long-term-stability study of Dox/Mito-DGL in RPMI 1640 or DMEM with 10% FBS.

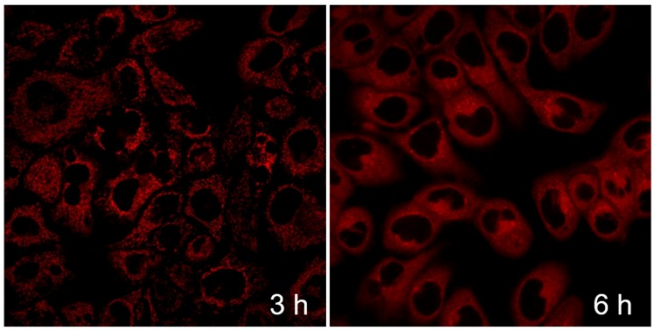

Figure S3. Confocal fluorescence imaging of HeLa cells incubated with 50 μg mL^{-1} Dox/Mito-DGL for 3 h and 6 h.

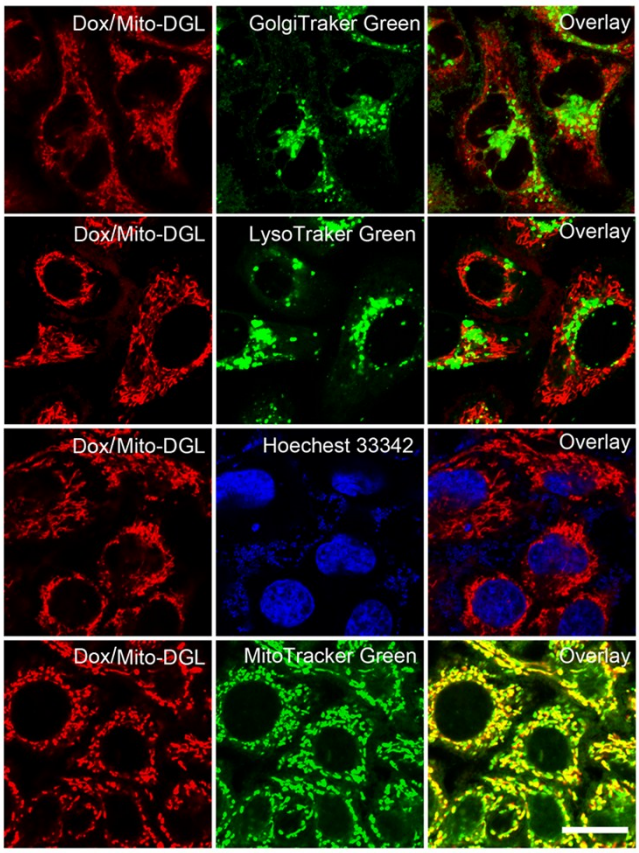

Figure S4. Colocalization images of Dox/Mito-DGL in PC3 cells. Cells incubated with the Dox/Mito-DGL for 3 h and then incubated with 50 nM LysoTracker Green, GolgiTracker Green, Hoechst 33342 and MitoTracker Green. Scale bars: 20 μm.

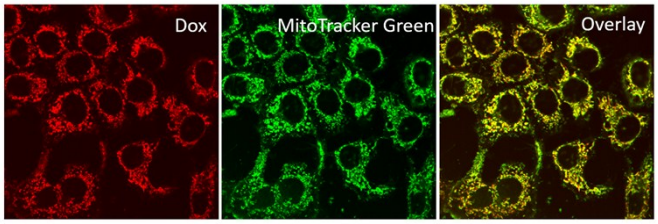

Figure S5. Confocal fluorescence images of the intracellular release of Dox from Dox/Mito-DGL: HeLa cells incubated with Dox/Mito-DGL for 4 h.

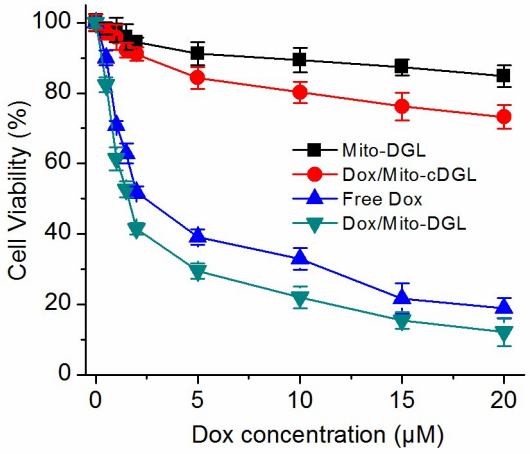

Figure S6. MTT assay of PC3 cells in the presence of different concentrations of Mito-DGL, Dox/Mito-cDGL, free Dox, and Dox/Mito-DGL.

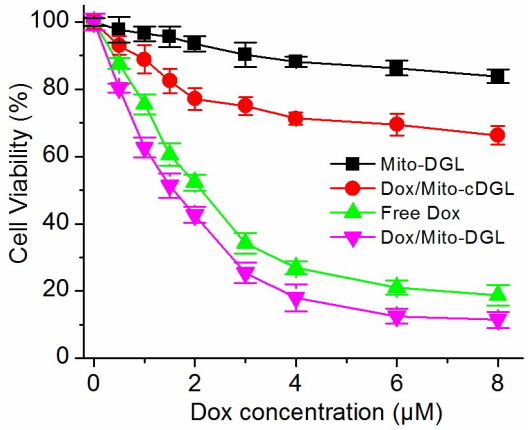

Figure S7. MTT assay of MCF-7 cells in the presence of different concentrations of Mito-DGL, Dox/Mito-cDGL, free Dox, and Dox/Mito-DGL.

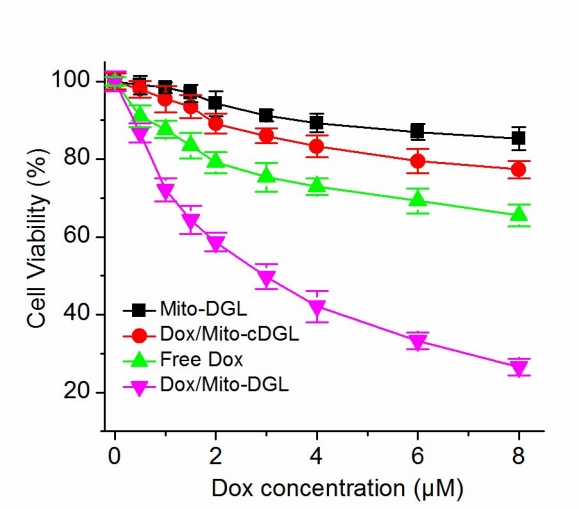

Figure S8. MTT assay of MCF-7/ADR cells in the presence of different concentrations of Mito-DGL, Dox/Mito-cDGL, free Dox, and Dox/Mito-DGL.

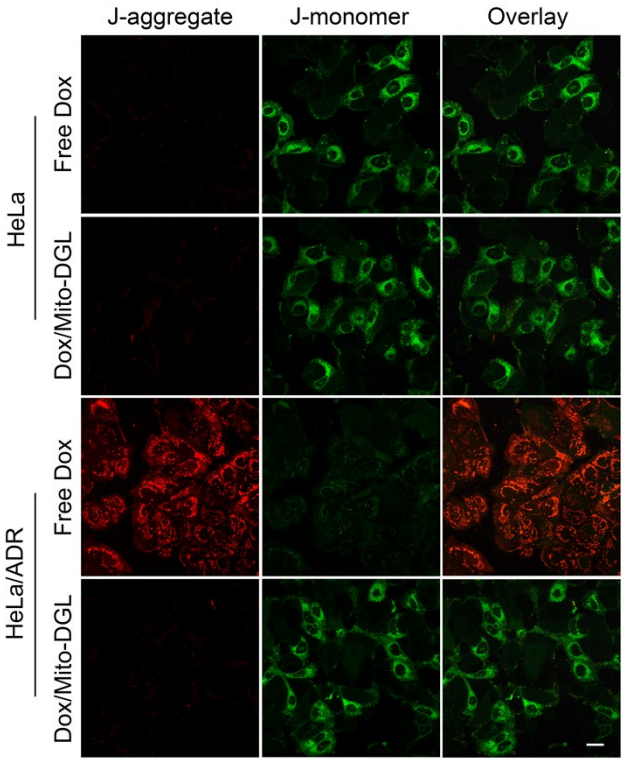

Figure S9. Confocal fluorescence images of apoptosis by the JC-1 assay in a) drug-sensitive HeLa and b) drug resistance HeLa/ADR cells treated with free Dox or Dox/Mito-DGL for 24 h. Scale bars: 20 μm.

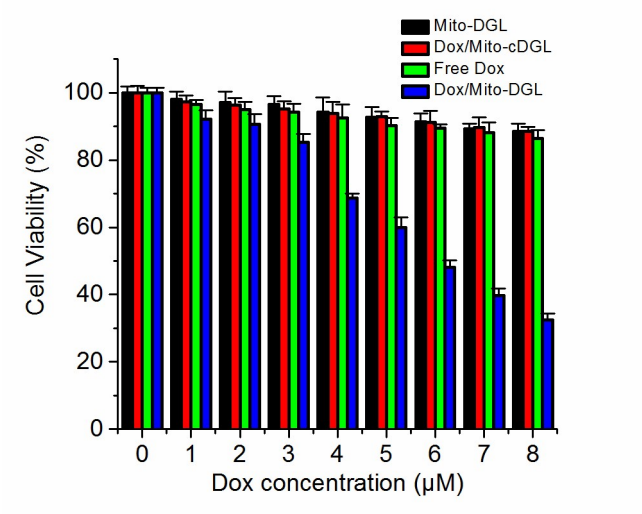

Figure S10. MTT assay of HeLa/ADR cells in the presence of different concentrations of Mito-DGL, Dox/Mito-cDGL, free Dox, and Dox/Mito-DGL.